Published OnlineFirst August 3, 2010; DOI: 10.1158/1535-7163.MCT-10-0190

Preclinical Development

Molecular Cancer Therapeutics

Dual Targeting of CDK and Tropomyosin Receptor Kinase Families by the Oral Inhibitor PHA-848125, an Agent with Broad-Spectrum Antitumor Efficacy

Clara Albanese[1], Rachele Alzani[1], Nadia Amboldi[1], Nilla Avanzi[1], Dario Ballinari[1], Maria Gabriella Brasca[1], Claudio Festuccia[2], Francesco Fiorentini[1], Giuseppe Locatelli[1], Wilma Pastori[1], Veronica Patton[1], Fulvia Roletto[1], Francesco Colotta[1], Arturo Galvani[1], Antonella Isacchi[1], Jurgen Moll[1], Enrico Pesenti[1], Ciro Mercurio[3], and Marina Ciomei[1]

Abstract

Altered expression and activity of cyclin-dependent kinase (CDK) and tropomyosin receptor kinase (TRK) families are observed in a wide variety of tumors. In those malignancies with aberrant CDK activation, the retinoblastoma protein (pRb) pathway is deregulated, leading to uncontrolled cell proliferation. Constitutive activation of TRKs is instead linked to cancer cell survival and dissemination. Here, we show that the novel small-molecule PHA-848125, a potent dual inhibitor of CDKs and TRKs, possesses significant antitumor activity. The compound inhibits cell proliferation of a wide panel of tumoral cell lines with submicromolar IC_{50}. PHA-848125–treated cells show cell cycle arrest in G_1 and reduced DNA synthesis, accompanied by inhibition of pRb phosphorylation and modulation of other CDK-dependent markers. The compound additionally inhibits phosphorylation of TRKA and its substrates in cells, which functionally express this receptor. Following oral administration, PHA-848125 has significant antitumor activity in various human xenografts and carcinogen-induced tumors as well as in disseminated primary leukemia models, with plasma concentrations in rodents in the same range as those found active in inhibiting cancer cell proliferation. Mechanism of action was also confirmed *in vivo* as assessed in tumor biopsies from treated mice. These results show that the dual CDK-TRK inhibitor PHA-848125 has the potential for being a novel and efficacious targeted drug for cancer treatment. *Mol Cancer Ther; 9(8); 2243–54. ©2010 AACR.*

Introduction

Cyclin-dependent kinases (CDK) are serine/threonine kinases that phosphorylate various proteins involved in the control of transcription and cell cycle progression (1). CDKs function in complex with activating partners, the cyclins, and are negatively regulated by natural inhibitory subunits, notably the CDK inhibitors (CDKI). Within the CDK family, CDK2, CDK4, and CDK6 are involved in several cell cycle processes during G_1 progression and DNA replication, whereas CDK7 has dual roles as a CDK-activating kinase and as a regulator of the transcriptional machinery. Other members, such as CDK8 and CDK9, seem to have key roles in the control of transcription by RNA polymerase II, whereas CDK10 and CDK11 exert their functions during the G_2-M transition and CDK1 is essential for cell division.

Deregulation of CDK activity has frequently been observed in cancer: It is estimated that altered expression levels and/or genetic mutations of cyclins, CDKs, or CDKIs, all components of the pRB/E2F pathway that controls G_1-S transition, are present in >90% of human neoplasms (2, 3). Cyclin D1 overexpression, for example, is found in leukemia, lymphomas, and multiple myeloma, as well as in many solid tumors (4). Cyclin E and A overexpression is reported in 50% of breast and lung cancer, whereas decreased levels of the CDKIs such as p27 predict poor prognosis in breast, prostate, colon, gastric, lung, and esophageal cancer (5–8).

Although several studies have shown that cells can tolerate targeted inhibition of a single CDK due to compensatory functions of the interphase kinases CDK2, CDK4, and CDK6 as shown using genetically engineered mice (9, 10), it nonetheless seems that specific genetic contexts in human tumors can generate dependence for specific CDKs (11, 12).

Thus, the biological roles played by CDKs in cell cycle proliferation, together with the observation of their frequent deregulation in human neoplasia, provide a

Authors' Affiliations: [1]BU Oncology, Nerviano Medical Sciences, Nerviano, Milan, Italy; [2]Experimental Medicine Department, University of L'Aquila, L'Aquila, Italy; and [3]Genextra Group, Milan, Italy

Note: Supplementary material for this article is available at Molecular Cancer Therapeutics Online (http://mct.aacrjournals.org/).

Corresponding Author: Clara Albanese, Cell Biology Department, BU Oncology, Nerviano Medical Sciences, v.le Pasteur 10, Nerviano, Milan 20014, Italy. Phone: 39-0331-581506; Fax: 39-0331-581374. E-mail: Clara.Albanese@nervianoms.com

doi: 10.1158/1535-7163.MCT-10-0190

Published OnlineFirst August 3, 2010; DOI: 10.1158/1535-7163.MCT-10-0190

rationale for their pharmacologic inhibition as a potential strategy in the treatment of human cancers, and it has been suggested that a broad spectrum of activity versus different CDKs could be advantageous to override potential compensatory and/or resistance-based mechanisms of cancer cells (13–15).

Recent years have consequently seen an intensive search for small molecules that target the CDKs, and many clinical trials have been conducted with both pan-CDKIs or with more selective compounds, but no CDKI has yet been approved for commercial use. Reasons for failure of the concluded studies described to date are unclear but have been suggested to include insufficient therapeutic window, inappropriate pharmacokinetic profile, and the difficulty in identifying patient populations potentially most sensitive to these agents (16).

The tropomyosin receptor kinase (TRK) subfamily of tyrosine kinases, comprising TRKA, TRKB, and TRKC, is a high-affinity receptor for the neurotrophin family of protein ligands, which include nerve growth factor (NGF) and brain-derived neurotrophic factor. Physiologically, the TRK/neurotrophin axis plays a role in neuronal maintenance and survival during development (17). TRK/neurotrophins have, however, also been implicated in cancer: Genetic rearrangement and activation of TRKA, for example, has been found in colon and papillary thyroid cancers (18), and of TRKC in several tumor types (19), whereas autocrine or paracrine activation of TRKs has been implicated in various cancers, including neuroblastoma, mesothelioma, pancreas, prostate, ovarian, and breast carcinomas (20–24).

We previously described optimization of a chemical class of CDK2 inhibitors, the 6-substituted pyrrolo[3,4-*c*] pyrazoles (25), and identification of a new orally available compound, PHA-848125 (26), which shows cross-reactivity toward CDK1, CDK4, CDK5, and CDK7. Differently from the other CDKIs, PHA-848125 is also highly potent toward TRKA and TRKC, supporting a rationale for testing this agent in selected cancer types where the neurotrophin/TRK receptor axis is thought to play a significant role.

Here, we describe the *in vitro* and *in vivo* pharmacologic profile of this dual CDK/TRK inhibitor.

Materials and Methods

Chemicals

PHA-848125, *N*,1,4,4-tetramethyl-8-{[4-(4-methylpiperazin-1-yl)phenyl]amino}-4,5-dihydro-1*H*-pyrazolo[4,3-*h*] quinazoline-3-carboxamide, was synthesized at Nerviano Medical Sciences, S.r.l.

PHA-848125 synthesis has been reported previously (26).

Biochemical kinase inhibition assays

Inhibition of kinase activity by PHA-848125 was assessed using a strong anion exchanger (Dowex 1X8 resin)–based assay in robotized format run on 384-well plates.

In this assay, specific peptides or protein substrates are transphosphorylated by their specific kinase in the presence of ATP traced with [γ-^{33}P]ATP using optimal buffers and cofactors.

The potency of the compound toward CDKs and 38 additional kinases belonging to an in-house Kinase Selectivity Screening panel was evaluated, and the relevant IC_{50}s were determined.

For each enzyme, the absolute K_M values for ATP and the specific substrate were calculated and each assay was then run at optimized ATP ($2K_M$) and substrate ($5K_M$) concentrations. This setting enabled direct comparison of IC_{50} values of PHA-848125 across the panel for the evaluation of its biochemical profile.

Cell culture

Human cancer cell lines were obtained either from the American Type Culture Collection or from the European Collection of Cell Culture. Cells were maintained in the media and serum concentrations recommended by the suppliers, supplemented with 1% penicillin-streptomycin (Sigma), in a humidified 37°C incubator with 5% CO_2. Routine characterization was done using AmpF*l*STR Identifiler PCR Amplification kit (Applied Biosystems). The cells were not tested and authenticated by an external service provider.

Analysis of cell proliferation

Cells were seeded into 96- or 384-well plates at densities ranging from 10,000 to 30,000/cm^2 in appropriate medium plus 10% FCS. After 24 hours, cells were treated in duplicate with serial dilutions of PHA-848125, and 72 hours later, viable cell number was assessed using the CellTiter-Glo Assay (Promega). IC_{50}s were calculated using a Sigmoidal fitting algorithm (Assay Explorer MDL). Experiments were done independently at least twice.

Cell-based mechanism assays

PHA-848125 mechanism of action as a CDKI was investigated using A2780 human ovarian carcinoma cells treated with the compound at the dose of 1 μmol/L for different times. Cells were analyzed by Western blot, immunocytochemistry, or flow cytometry, measuring cell cycle–dependent parameters and DNA synthesis.

PHA-848125 activity on the TRKA signaling pathway was specifically evaluated on the DU-145 human prostate carcinoma cell line, which functionally expresses this kinase (27). DU-145 cells were serum starved for 16 hours, then treated with the compound at the indicated concentrations for 30 minutes, and finally stimulated with 50 ng/mL NGF for 15 minutes.

Western blot analysis

Cells extracts were prepared in lysis buffer containing 125 mmol/L Tris-HCl (pH 6.8) and 5% (w/v) SDS. Samples were heated at 95°C for 5 minutes and then sonicated.

Published OnlineFirst August 3, 2010; DOI: 10.1158/1535-7163.MCT-10-0190

Protein extract (20 μg for A2780 or 80 μg for DU-145), as determined by bicinchoninic acid protein assay (Pierce), was loaded and separated by SDS-PAGE in 8% bis/acrylamide gels. Immunoblotting was done according to standard procedures, and staining was done with the following antibodies against: retinoblastoma protein (pRb), cyclin B1, cyclin D1, cyclin A, and Kip/p27 (Pharmingen-BD Biosciences); Cdc6 (NeoMarkers); p53, Cdc25A, TRKA, and phospho-TRKA (Santa Cruz Biotechnology); pRb-phospho-Thr^{821} and pRb-phospho-Ser$^{249/252}$ (Biosource); and pRb-phospho-Ser^{780}, pRb-phospho-Ser$^{807/811}$, phospho-phospholipase Cγ, phospho-AKT, and total AKT (Cell Signaling). SuperSignal Chemiluminescence kit (Pierce) was used for detection.

Cell cycle analysis

Cells were collected, fixed, and stained as previously described (28). Cytofluorimetric analysis was done using a FACSCalibur (BD Biosciences), and cell cycle phases were calculated by ModFit 3.0 (Verity Software House).

Immunocytochemical analysis

Exponentially growing cells treated with compound were pulsed with 50 μmol/L bromodeoxyuridine (BrdUrd; Sigma) for 60 minutes, collected, and cytospun onto slides. Staining was done as previously described (28). Percentage of BrdUrd incorporation was calculated counting positive nuclei from a total of 200 cells.

Animal efficacy studies

All procedures adopted for housing and handling of animals were in strict compliance with European and Italian Guidelines for Laboratory Animal Welfare. For tumor xenograft studies, female Hsd, athymic *nu/nu* mice (Harlan), ages 5 to 6 weeks (average weight, 20–22 g), were used. A2780 ovarian carcinoma; HCT116 colon carcinoma; BX-PC3, MiaPaca, and CAPAN-1 pancreatic carcinomas; DU-145 prostatic carcinoma; A549 non–small cell lung cancer; and A375 melanoma human cell lines were transplanted s.c. in athymic mice. Mice bearing a palpable tumor (100–200 mm^3) were randomized into vehicle and treated groups. Treatments, at doses and scheduling indicated in Fig. 3A and Supplementary Table S4, started the day after randomization. Tumor dimensions were measured regularly using Vernier calipers, and tumor growth inhibition (TGI) was calculated as previously described (29).

Toxicity was evaluated based on body weight reduction. At the end of the experiment, mice were sacrificed and gross autopsy findings were reported. For the leukemia studies, female severe combined immunodeficient (SCID) mice (Harlan), ages 5 to 6 weeks (average weight, 20–22 g) were used. In the case of HL60, 5×10^6 cells were injected s.c. to obtain growth as a solid tumor, and treatment initiated when tumor size reached 200 to 250 mm^3. Tumor dimensions were monitored during the experiment and TGI was assessed as described above. In the case of disseminated acute myelogenous leukemia (AML) and acute lymphoblastic leukemia (ALL) models, mice were injected i.v. with 5×10^6 leukemic cells and treatment with PHA-848125 was initiated after 2 days. Mice were monitored daily for clinical signs of disease, and deaths were recorded for calculation of the median survival time.

Treatment of rats with established 7, 12-dimethylbenz(a)anthracene–induced mammary tumors

Tumor induction was done as previously described (29). Rats were randomized and introduced into the study when at least one mammary tumor attained a diameter of 0.5 cm. Groups of 10 animals were treated orally twice a day continuously for 10 days with vehicle (glucosate) or with 5, 10, and 15 mg/kg of PHA-848125, whereas a further group received two cycles of PHA-848125 at 20 mg/kg orally twice a day for 5 days with an intervening rest period of 1 week. Tumor volume was measured regularly by caliper for the duration of the experiment.

Ex vivo mechanism of action studies

A2780 tumor-bearing mice were treated with 40 mg/kg PHA-848125 (in glucosate) orally twice a day for 1 and 5 days. Tumors from treated or vehicle animals (five per group) were collected 90 minutes after the last administration and subdivided by scalpel. Two fragments from each tumor were immediately placed in formalin for immunohistochemistry and a third in RNAlater solution (Qiagen) for quantitative real-time PCR (RT-PCR) analysis.

Immunohistochemistry

Tumors were fixed in 10% buffered formalin for 24 hours and paraffin embedded. Immunohistochemistry was done as previously described (30). Briefly, serial sections were unmasked in citrate buffer (pH 6) by pressure cooker and incubated with rabbit polyclonal antibody against pRb-phospho-Thr^{821} (Biosource) and mouse monoclonal antibody against cyclin A (Novocastra Laboratories) for 2 hours and 1 hour, respectively, at room temperature. Dako EnVision System HRP for rabbit or mouse was used as secondary antibody. All slides were incubated with DAB Substrate Chromogen System (Dako). Histologic examination was done on H&E-stained sections.

Image analysis

Sections were examined in blind by two independent observers using a Zeiss microscope (Axioscope-2 plus) equipped with a charge-coupled device camera (Evolution MP-Color, Media Cybernetics). Quantification of cyclin A– and pRb-positive cells in tumors was done in viable areas using Image-Pro Plus software (Media Cybernetics). Ten fields (at 10× objective for cyclin A) and 6 fields (at 20× objective for pRb) were collected and analyzed. Results are reported as the mean of

Published OnlineFirst August 3, 2010; DOI: 10.1158/1535-7163.MCT-10-0190

positive cells per field per sample. The Mann-Whitney test was used for statistical analysis.

RT-PCR studies

Total RNA was extracted using the Qiagen RNeasy kit, starting from 20 mg of tumor tissue following the manufacturer's instructions. RNA quality/quantity was assessed by UV absorbance at 260 and 280 nm and visual inspection following electrophoresis in Tris-borate EDTA/1.5% agarose gels and ethidium bromide staining.

Total RNA was retrotranscribed using the Applied Biosystems Reverse Transcription kit following the manufacturer's instructions in a final reaction volume of 25 μL; the resulting cDNA was diluted in Tris-EDTA buffer to a final concentration of 5 mg/mL before PCR amplification on the ABI Prism 7900 thermal cycler. RT-PCR was done using Applied Biosystems SYBR Green MasterMix 1×, with 300 nmol/L primers and 12.5 ng of cDNA in 12.5 μL of reaction volume; the reaction started with 10 minutes at 95°C, followed by 40 cycles of 15 seconds at 95°C/45 seconds at 60°C.

PCR primers were selected to specifically amplify fragments of human *Rrn 18s, Actb, Ppia*, and *Gusb* (housekeeping genes), and CDK2/pRB/E2F pathway readout genes using Applied Biosystems Primer Express Software (Supplementary Table S1) and synthesized in house. Specificity of primers, whose sequence was designed in correspondence with exon junctions conserved in all known alternative spliced forms, was verified against the National Center for Biotechnology Information GenBank database using the Blast algorithm.

RT-PCR data quantitative analysis

Analysis of RT-PCR output data used the manufacturer-recommended $-\Delta\Delta C_t$ method, which provides the target gene expression value as unitless fold change in the unknown sample compared with a calibrator sample; both unknown and calibrator sample target gene expressions were normalized to housekeeping gene expression levels (average of *Rrn 18s, Actb, Ppia*, and *Gusb*).

The calibrator sample was obtained by retrotranscription of an equal mix of the 12 human tissue RNA samples contained in the Panel I and IV tissue mRNA collections from Clontech.

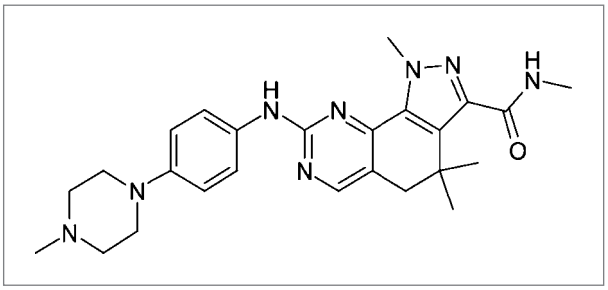

Figure 1. Chemical structure of PHA-848125 (*N*,1,4,4-tetramethyl-8-{[4-(4-methylpiperazin-1-yl)phenyl]amino}-4,5-dihydro-1*H*-pyrazolo[4,3-*h*]quinazoline-3-carboxamide).

Table 1. Kinase inhibition profile of PHA-848125

Kinase	IC_{50} (nmol/L)
CDK2/cyA	45
CDK/cyH	150
CDK4/cyD	160
CDK5/p25	265
CDK2/cyE	363
CDK1/cyB	398
TRKA	53
	85*
TRKC	134*
TRKB	745*
LCK	209
ABL	478
PDGFR	579
KIT	668

NOTE: IC_{50}, the concentration of PHA-848125 inducing 50% inhibition of kinase activity.
*Obtained from Invitrogen SelectScreen Kinase Profiling Service.

Pharmacokinetics and pharmacodynamics

Pharmacokinetic properties of PHA-848125 were investigated in mouse (*nu/nu*), rat (Han Wistar), beagle dog, and cynomolgus monkey after single intravenous and oral administration at the doses of 10 mg/kg (mouse and rat) and 5 mg/kg (monkey and dog).

Plasma levels of PHA-848125 were determined by protein precipitation in a 96-well plate format followed by liquid chromatography–tandem mass spectrometry. In all animal species, the lower and upper limits of quantification were 1 and 1,000 ng/mL. Pharmacokinetic data analysis was carried out using a noncompartmental approach (linear trapezoidal rule) with the aid of WinNonlin (v3.1; Pharsight, Inc.).

The pharmacokinetic/pharmacodynamic analysis was done using the previously described method (31) in an ancillary group of three A2780 tumor-bearing mice. Compartmental analysis was done using a one-compartment model with first-order administration and elimination.

Results

Kinase inhibition

PHA-848125 is a pyrazolo[4,3-*h*]quinazoline (Fig. 1), which potently inhibits the kinase activity of CDK2/cyclin A complex and of TRKA in a biochemical assay, with IC_{50}s of 45 and 53 nmol/L, respectively (Table 1). Cross-reactivity with other CDKs (i.e., CDK1, CDK4, CDK5, and CDK7) was seen at 4- to 10-fold higher IC_{50}s compared with CDK2, and a similar potency was

Published OnlineFirst August 3, 2010; DOI: 10.1158/1535-7163.MCT-10-0190

also observed toward other cancer-related kinases [such as KIT, ABL, and platelet-derived growth factor receptor (PDGFR)]. A panel of 35 other kinases representative of the human kinome superfamilies displayed IC_{50}s higher than 1 μmol/L (Supplementary Table S2), among these were CDK9/cyclinT, as well as several mitotic kinases (Aurora A and B, PLK1, NEK6, and MPS1). To investigate potency toward other members of TRK family, the compound was tested through the Invitrogen SelectScreen Kinase Profiling Service, and the resulting IC_{50}s were as follows: 85 nmol/L for TRKA (comparable with in-house results), 745 nmol/L for TRKB, and 134 nmol/L for TRKC. Based on these data, PHA-848125 can be defined as a selective dual inhibitor of the CDK and TRK families.

Effect on tumor cell proliferation and mechanism of action

The antiproliferative activity of PHA-848125 was tested in 72-hour proliferation assays against a panel of 145 tumor cell lines established from different solid tumors and a further 44 cell lines derived from leukemias and lymphomas (Supplementary Table S3). IC_{50} values were below 1 μmol/L (Fig. 2A; Supplementary Table S4) for 96 cell lines (including 6 of 6 ALL, 8 of 12 AML, 12 of 14 lymphoma, 16 of 26 colon, 8 of 8 kidney, 6 of 8 ovary, 11 of 24 non–small cell lung, 2 of 2 neuroblastoma, 2 of 2 osteosarcoma, and 2 of 2 thyroid) and higher than 1 μmol/L (Fig. 2B; Supplementary Table S4) for 93 cell lines, indicating a broad spectrum of activity. Only nine cell lines were poorly responsive (i.e., with an IC_{50} value of >5 μmol/L). Compound activity was not significantly affected by P-glycoprotein overexpression (e.g., IC_{50} of 0.20 and 0.24 μmol/L on A2780 and A2780/ADR, respectively), DNA repair deficiency (e.g., IC_{50} of 0.20 and 0.25 μmol/L on A2780 and A2780/cis, respectively), pRb status (e.g., IC_{50} of 0.46 and 1.11 μmol/L on BT-549 and MDA-MB-468, both Rb-null cell lines), or p53 activity (e.g., IC_{50} of 0.20 and 0.10 μmol/L on A2780 and A2780/E6, respectively). Among the most sensitive cell lines, there were cells whose growth might depend also on one of the non-CDK kinases inhibited by PHA-848125: the Bcr-Abl–positive KU812 chronic myeloid leukemia cell line (IC_{50}, 0.004 μmol/L), the TRKAIIIsplice variant-expressing

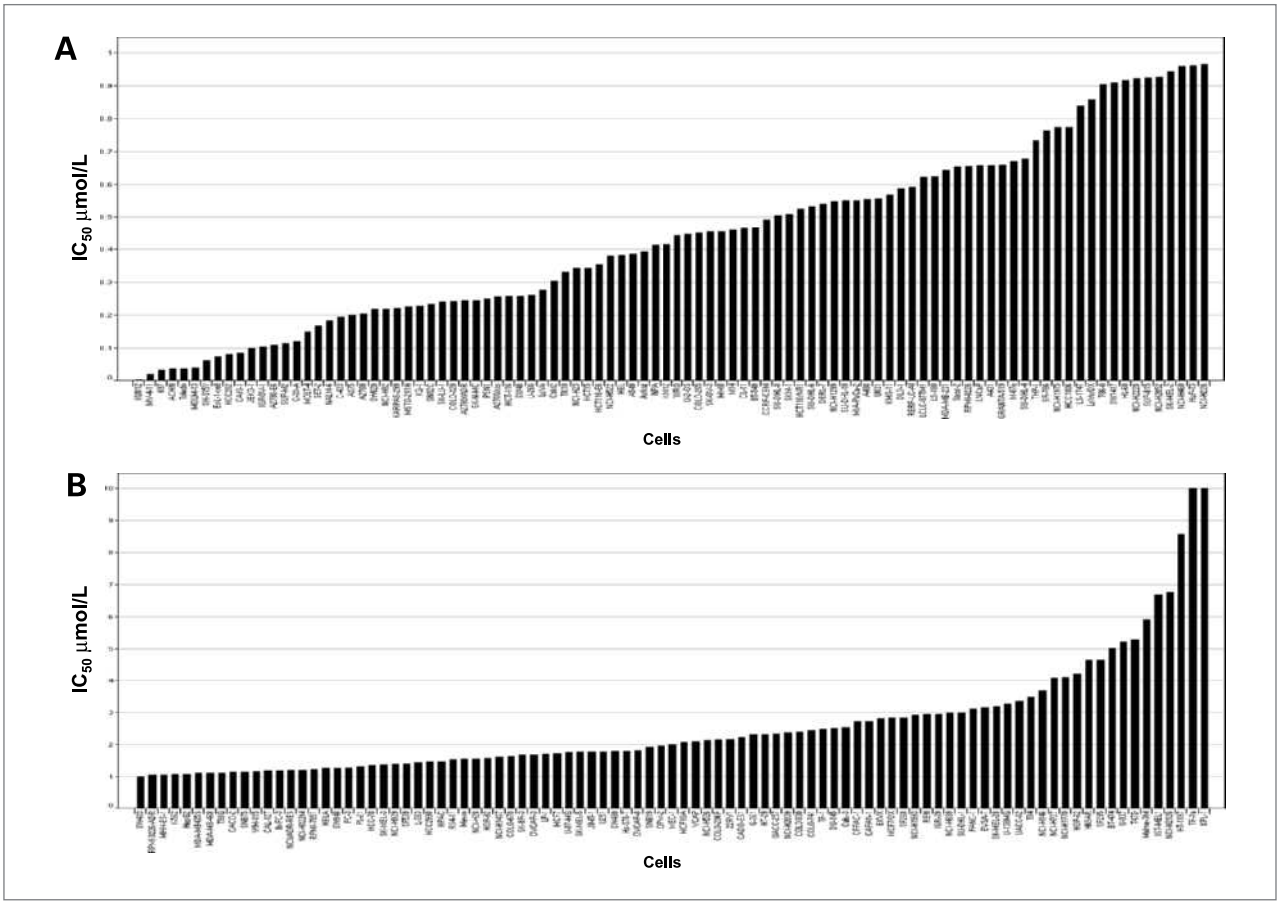

Figure 2. Inhibition of cell proliferation after treatment with PHA-848125. The compound was tested on a panel of 189 different cell lines in a wide range of doses to reliably calculate the IC_{50}. A, bar chart indicating the cell lines having IC_{50} lower than 1 μmol/L. B, bar chart indicating the cell lines having IC_{50} higher than 1 μmol/L.

Published OnlineFirst August 3, 2010; DOI: 10.1158/1535-7163.MCT-10-0190

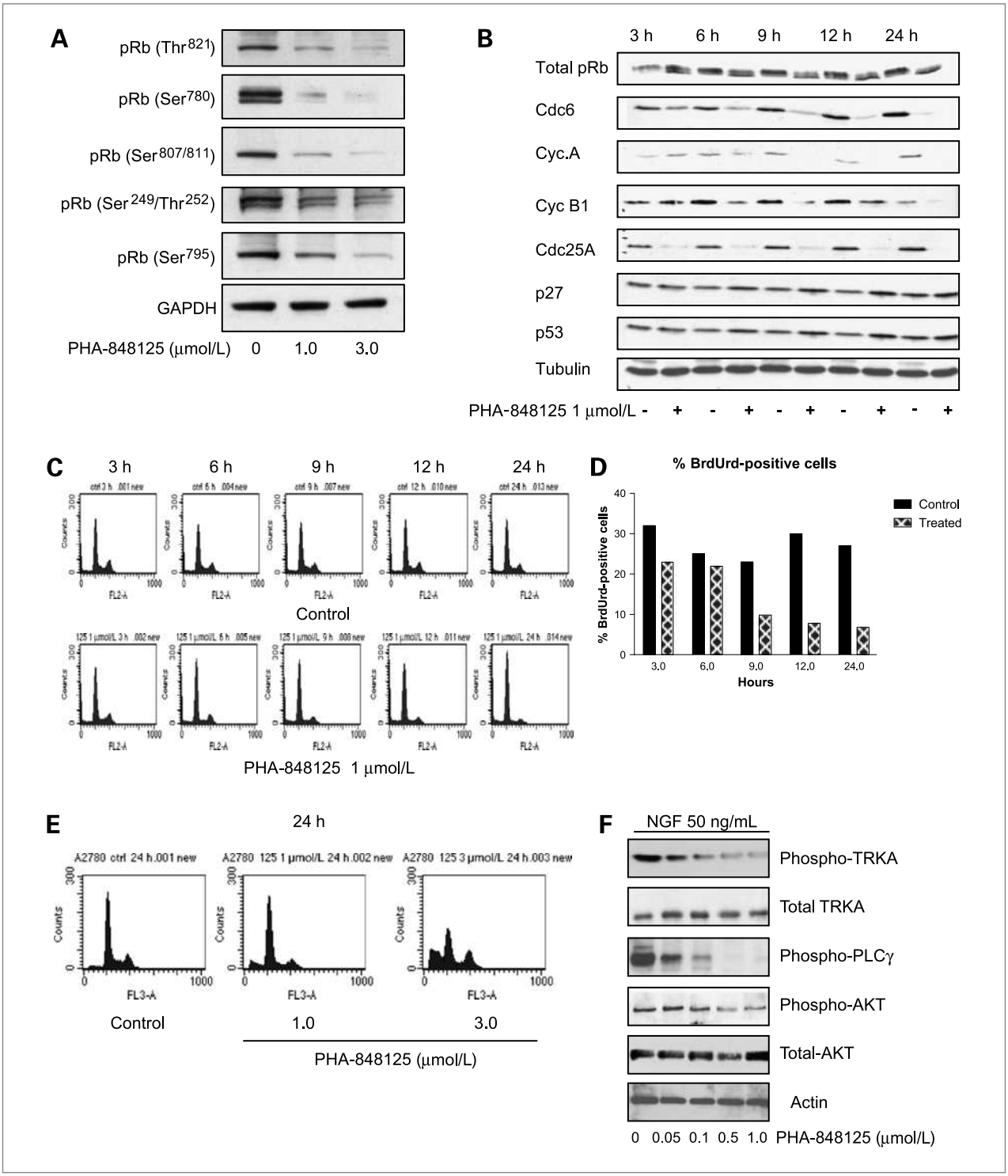

Figure 3. A, effect of PHA-848125 on phosphorylation status of pRb. A2780 cells were treated for 24 h with 1 and 3 μmol/L PHA-848125. Total cell lysates were immunoblotted and the different sites of phosphorylation were probed with specific antibodies. B, effect of PHA-848125 on several CDK-related proteins. A2780 cells were treated with 1 μmol/L PHA-848125 for indicated times. Total cell lysates were immunoblotted with specific antibodies. C, cell cycle distribution of A2780 cells treated with 1 μmol/L PHA-848125 was determined by flow cytometry at different time points and compared with the corresponding control cells. D, the same samples used for cell cycle evaluation were analyzed by immunocytochemical staining for BrdUrd incorporation to quantify DNA replication. E, cell cycle distribution of A2780 cells, untreated or treated with 1 and 3 μmol/L PHA-848125 for 24 h. F, effect of PHA-848125 on TRKA phosphorylation and downstream pathway. DU-145 cells were serum starved and pretreated with different doses of the compound for 30 min before NGF stimulation for 15 min. Total cell lysates were immunoblotted with specific antibodies.

Published OnlineFirst August 3, 2010; DOI: 10.1158/1535-7163.MCT-10-0190

SH-SY5Y neuroblastoma (IC_{50}, 0.064 μmol/L), and the FIP1L1-PDGFR–expressing EoL-1 AML cell line (IC_{50}, 0.075 μmol/L). For these cell lines, the inhibition of proliferation could result from the dual effect of the compound on CDKs and on the respective tyrosine kinase.

The mechanism of action of the compound was tested on several cell lines, showing in all of them a homogeneous behavior in terms of cell cycle– and target-related signaling modulation. Figure 3 shows the results obtained on A2780, where treatment with PHA-848125 for 24 hours induced a strong dose-dependent inhibition of all the major phosphorylation sites of pRb known to be CDK2, CDK4, and CDK1 substrates (Fig. 3A).

In time course studies (Fig. 3B), hypophosphorylation of pRb was already discernible at 1 μmol/L and 6 hours of treatment. At the same dose and time of exposure, decrease of cyclin A (complexed by both CDK2 and CDK1) and of cyclin B1 (a specific cofactor of CDK1) was evident, concomitant with an increase in p27 and p53 expression, which are involved in cell cycle arrest and/or apoptosis. Decrease of both Cdc6 and Cdc25A, factors required for S-phase entry, was the earliest event, already evident at 3 hours.

As a consequence, 1 μmol/L PHA-848125 induced a clear accumulation of cells in G_1 phase, maximal at 24 hours (86% in treated cells versus 60% in control cells), and concomitant with a decrease of cells in S phase (9% in treated cells versus 25% in control cells; Fig. 3C) and with marked reduction in active DNA synthesis as measured by BrdUrd incorporation (Fig. 3D). At the dose of 3 μmol/L for 24 hours, cells accumulated in G_2-M (27% in treated cells versus 11% in control cells) and a 10-fold increase of cells with sub-G_1 DNA content was evident compared with controls, suggesting induction of cell death and apoptosis (Fig. 3E).

Among the different cell lines on which the mechanism of action of the compound was tested, DU-145 cells (Supplementary Fig. S1), having TRKA functionally expressed, were used to show the dual inhibition. A short treatment of 30 minutes with PHA-848125 was sufficient to strongly inhibit NGF-induced phosphorylation of this kinase in a dose-dependent manner, whereas total protein was unaffected. This inhibition also coincided with reduced levels of the downstream signaling components phospho-phospholipase Cγ and phospho-AKT (Fig. 3F).

Antitumor activity *in vivo*

Because the pharmacokinetic properties of PHA-848125 were suitable for preclinical *in vivo* studies, the efficacy of the compound was tested in a wide range of human xenograft tumors s.c. implanted in athymic mice. In these studies, a daily twice a day oral treatment was administered for a maximum of 10 days. As shown in Table 2, the compound was effective, with maximal TGIs ranging from 64% to 91% (a representative TGI curve is reported in Fig. 4A), and well tolerated (body weight loss from 0% to 15%) in all tested models at the optimal dose of 40 mg/kg twice a day, selected on the basis of a previous dose-response experiment on A2780 xenografts (26). The human prostate DU-145 model, with nonfunctional Rb, but expressing TRKA, was among the highly sensitive models.

We extended our study to the 7,12-dimethylbenz(a) anthracene (DMBA)–induced rat mammary carcinoma model, which resembles human breast carcinoma and potentially represents a biologically relevant syngeneic model to test the activity of CDK2 inhibitors, given the cyclin E overexpression and reduced p27 expression reported for these tumors (32). PHA-848125 was administered by oral route at doses of 5, 10, and 15 mg/kg for 10 days twice a day (Fig. 4B). At the lower doses, tumor stasis was observed (16% at 5 mg/kg and 50% at 10 mg/kg), whereas at 15 mg/kg, regression in 50% of the primary tumors was also seen (Fig. 4B).

A cyclic intermittent treatment schedule was also tested in the same model. PHA-848125 was administered

Table 2. *In vivo* activity of PHA-848125 in human xenograft tumor models

Model	Dose/schedule (mg/kg twice a day/D1–D10)	Maximal % TGI (day)	Maximal weight loss (%)
A2780 ovarian cancer (nude mice)	40	91% (11)	10
HL60 AML (SCID mice)	40	84% (11)	9
HCT116 colon cancer (nude mice)	40	64% (11)	15
BX-PC3 pancreatic cancer (nude mice)	40	74% (10)	10
CAPAN-1 pancreatic cancer (nude mice)	40	65% (11)	11
DU-145 prostatic cancer (nude mice)	40	91% (11)	0
A375 melanoma (nude mice)	40	69% (11)	9
A549 non–small cell lung cancer (nude mice)	40	73% (11)	0
MiaPaca-2 pancreatic adenocarcinoma (nude mice)	40	70% (11)	0

NOTE: The compound was administered twice a day at 40 mg/kg for 10 consecutive days (D1–D10). Percentage of inhibition compared with the vehicle-treated group and the maximal weight loss were calculated 1 d after the stop of treatment.

Published OnlineFirst August 3, 2010; DOI: 10.1158/1535-7163.MCT-10-0190

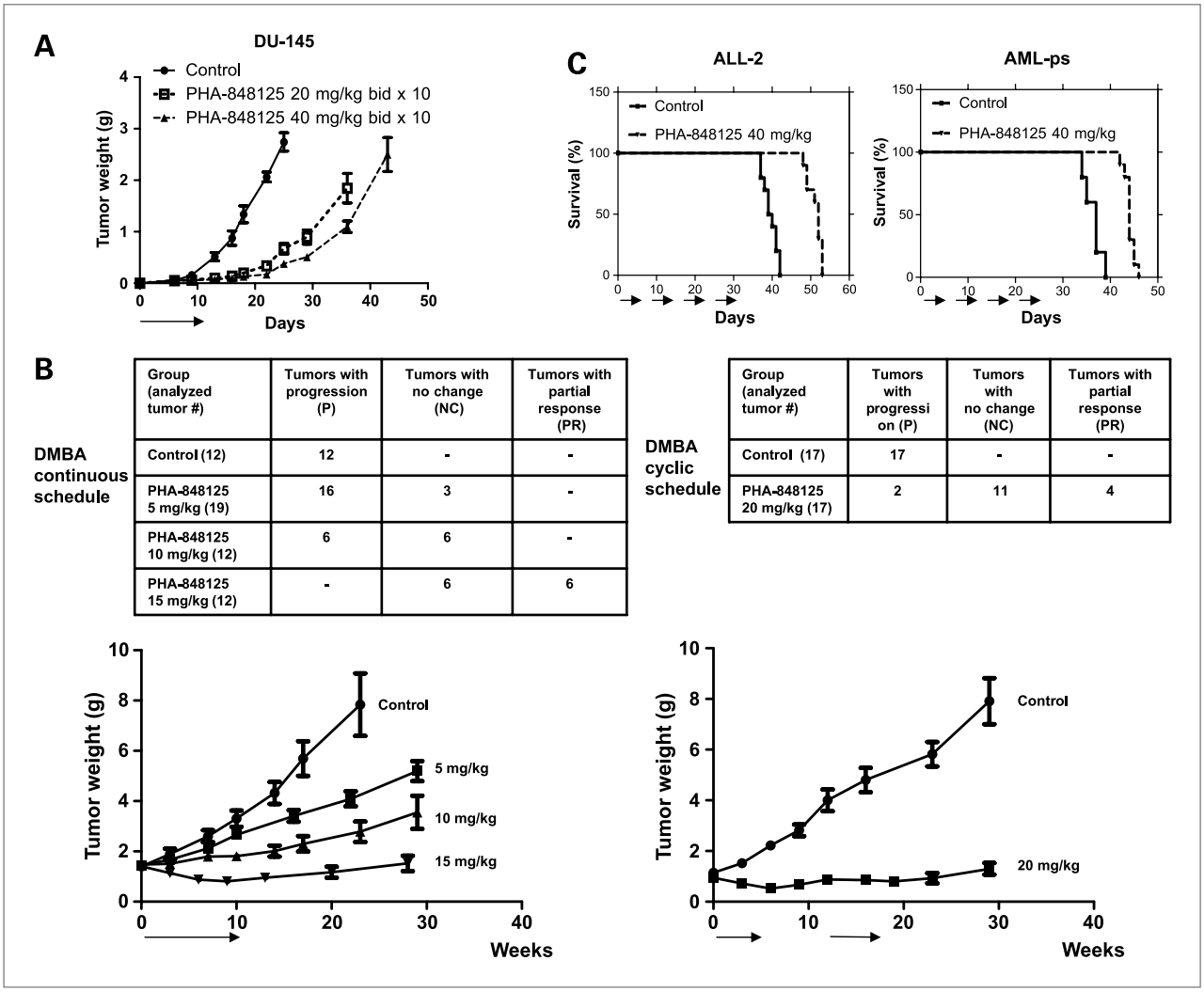

Group (analyzed tumor #)	Tumors with progression (P)	Tumors with no change (NC)	Tumors with partial response (PR)
Control (12)	12	-	-
PHA-848125 5 mg/kg (19)	16	3	-
PHA-848125 10 mg/kg (12)	6	6	-
PHA-848125 15 mg/kg (12)	-	6	6

Group (analyzed tumor #)	Tumors with progression (P)	Tumors with no change (NC)	Tumors with partial response (PR)
Control (17)	17	-	-
PHA-848125 20 mg/kg (17)	2	11	4

Figure 4. *In vivo* efficacy of PHA-848125. A, DU-145 xenograft tumor, inoculated s.c. B, DMBA-induced mammary tumors. Two different schedules were tested: continuous (10 d) or cyclic (two cycles of 5 d). In the inserted tables, results are expressed in terms of tumor progression or regression. C, ALL-2 disseminated human ALL and AML-ps disseminated AML. PHA-848125 was administered at the indicated doses. Arrows, dosing period. Bars, SD.

at 20 mg/kg twice a day for 5 days, repeated after an intervening rest period of 8 days (for a total of 10 days of treatment). This intermittent treatment gave TGI comparable with that observed with continued daily dosing for 10 days at 15 mg/kg, suggesting schedule independency of the compound (Fig. 4B).

On the basis of the significant TGI obtained in the s.c. implanted HL60 human leukemia model, PHA-848125 efficacy was also explored in two models of human primary disseminated leukemias, which might more closely reflect the pathogenesis of the human disease: ALL-2 derived from a Philadelphia chromosome–positive ALL patient in relapse (33) and AML-ps derived from an AML patient with normal karyotype (34).

As shown in Fig. 4C, in both models, PHA-848125 at 40 mg/kg orally twice a day × 5 days, repeated for four cycles, showed a significant increase ($P < 0.0001$) in median survival time when compared with vehicle: 52 days versus 39.5 days for ALL-2 and 44 days versus 37 days for AML-ps.

In vivo mechanism of action

To show that PHA-848125 is also able to inhibit CDK activity *in vivo* and to correlate mechanism of action with the suppression of tumor growth, A2780 xenograft tumors were collected after 1 and 5 days of oral treatment at 40 mg/kg twice a day. Phosphorylation of pRb was assayed by immunohistochemistry using an antibody specific for phospho-Thr^{821}, a direct CDK2 substrate. One day of treatment was sufficient to induce a statistically significant reduction of pRb-positive cells, which persisted after 5 days of treatment (Fig. 5A; Supplementary Fig. S2), when TGI was 60%. Similar

Published OnlineFirst August 3, 2010; DOI: 10.1158/1535-7163.MCT-10-0190

results were also obtained using a phospho-Ser$^{807/811}$–specific antibody, which recognizes a site on pRb that has been linked to CDK4 activity (Supplementary Fig. S2). Concomitantly, the fraction of cells positive for cyclin A, one of the proteins directly regulated by CDK2 and *CDK1*, was also significantly reduced, as expected (Fig. 5A; Supplementary Fig. S2). Levels of proliferation as measured by BrdUrd incorporation (Supplementary Fig. S2) were also monitored by immunohistochemistry and were decreased, in accordance with the findings for phospho-pRb and cyclin A. On the same tumors tested by immunohistochemistry, gene expression analysis was carried out by RT-PCR on 20 genes regulated by the CDK2/pRB/E2F pathway, and whose expression should be negatively modulated by CDK inhibition; this analysis showed that 17 of 20 genes were significantly downmodulated ($P < 0.05$) by PHA-848125 after 1 day of treatment and 13 of 20 remained downmodulated after 5 days of treatment (Fig. 5B). These results correlated well with immunohistochemical data and together confirmed PHA-848125 mechanism of action as regards CDK inhibition. TRKA inhibition *in vivo* was not demonstrable in this tumor model because A2780 cells express inadequate levels of this kinase.

Pharmacokinetics and pharmacodynamics

Pharmacokinetic parameters were measured in mouse, rat, dog, and monkey (Table 3). After intravenous administration, the compound showed moderate plasma clearance accounting for approximately 36%, 47%, 76%, and 43% of the hepatic blood flow, respectively (35). The volume of distribution was high in all species, suggesting extensive tissue distribution, as was oral bioavailability, with F = 80%, 66%, 59%, and 30% in mouse, rat, dog, and monkey, respectively.

A pharmacokinetic and pharmacodynamic approach, based on a previously described model (31), was applied to the efficacy data obtained in A2780 tumor-bearing mice. This method, linking plasma concentrations of the anticancer compound under test to effects on tumor growth, provides quantitative estimates of *in vivo* potency through the determination of two model parameters: K_2 and C_t. K_2 is the proportionality factor linking plasma concentration to effect and can be regarded as a drug-specific measurement of potency of the compound. The C_t value provides an estimate of the steady-state drug concentration in plasma required for observing tumor regression and eventually tumor eradication. The estimated C_t value for PHA-848125 in the A2780 model was ~2.4 μmol/L (Fig. 6).

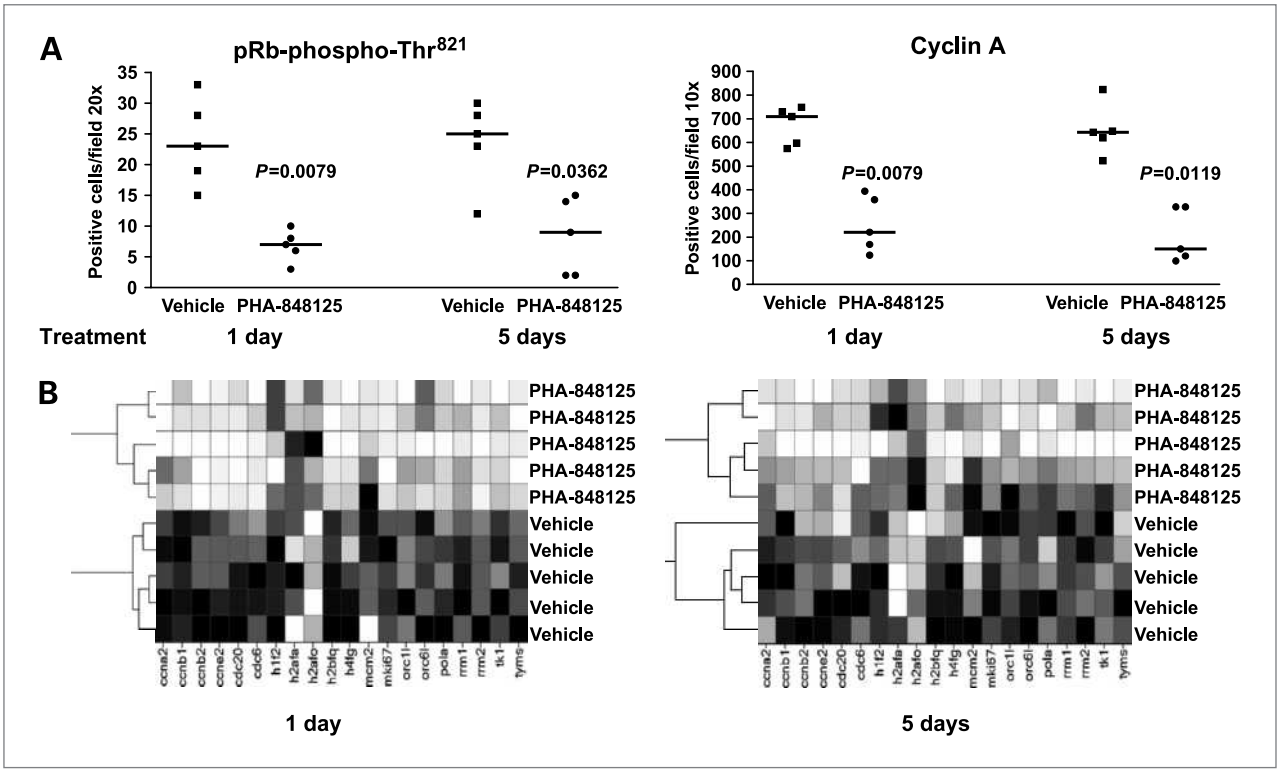

Figure 5. *In vivo* mechanism of action of PHA-848125. A2780 xenografted tumors were analyzed after treatment with PHA-848125 at 40 mg/kg twice a day for 1 and 5 d by immunohistochemistry (A) and RT-PCR (B). A, quantitative analysis of vehicle and treated tumors immunostained with anti–pRb-phospho-Thr^{821} and anti–cyclin A. ■, vehicle; ●, PHA-848125–treated tumors. Bar, median of the group. B, hierarchical clustering based on gene expression of 20 CDK2/Rb/E2F-regulated genes in vehicle and treated tumors. Clustering method, Unweighted Pair Group Method with Arithmetic mean (UPGMA) unweighted average; similarity measure, correlation; ordering function, average value.

Published OnlineFirst August 3, 2010; DOI: 10.1158/1535-7163.MCT-10-0190

Table 3. Mean pharmacokinetic parameters of PHA-848125 in preclinical species

Species	Gender	$t_{1/2}$ (h)	CL (L/h/kg)	V_{ss} (L/kg)	*F* (%)
Mouse	M	1.9	1.8	3.5	80
Rat	M	3.4	1.9	7.5	66
Dog	M/F	6.7	1.9	12	59
Monkey	M/F	4.1	1.4	5.3	30

Discussion

The dearth of clinical success to date of selective CDKIs indicates that a compound possessing a broad spectrum of activity versus different CDKs could be advantageous to bypass potential compensatory and/or resistance-based mechanisms of cancer cells (9, 10, 15). Indeed, the pyrazolo quinazoline compound PHA-848125 presented here showed *in vitro* activity against most of CDK family members, in particular against CDK2/cyclin A and CDK4/cyclin D complexes.

PHA-848125 exhibited strong antiproliferative activity (IC_{50} in the nanomolar range for ~50% of 189 tested lines) independently of status of P-glycoprotein, p53, and DNA damage repair proficiency.

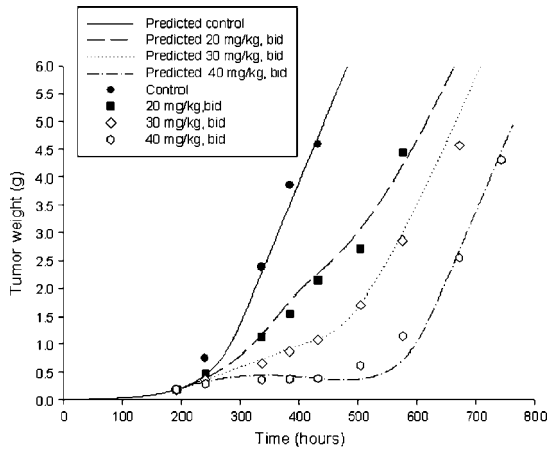

Parameters	Estimates	CV%
K_1 (day^{-1})	0.394	21.6
K_2 (μmol/L^{-1} mL day^{-1})	0.190	7.96
λ_0 (day^{-1})	0.445	5.80
λ_1 (day^{-1})	0.605	4.78
L_0 (g)	0.005	24.7
C_t (μmol/L)	2.34	4.81
C_t unbound (μmol/L)	0.293	

Figure 6. Pharmacokinetic/pharmacodynamic model: observed and predicted tumor weight model-fitted tumor growth curves obtained in nude mice bearing A2780 xenograft tumor treated orally with vehicle (control) or PHA-848125 at 20, 30, and 40 mg/kg twice a day for 10 d. In the inserted table, model parameters are reported.

The mechanism of action of the drug was shown in A2780 cells, where doses that inhibited growth at 72 hours were able at early time points to inhibit phosphorylation of pRb and to downmodulate expression of CDK-dependent genes. Phosphorylation sites of pRb particularly sensitive to PHA-848125 included Thr^{821}, Ser^{780}, and $Ser^{807/811}$, which are specific for CDK2 and CDK4 activity and which regulate interaction with transcription factors such as E2F, essential for the transition from G_1 to S phase (36, 37). Consequently, low doses of PHA-848125 strongly reduced DNA replication (as confirmed by robust inhibition of BrdUrd incorporation) and induced G_1 block. At higher drug doses, the accumulation of cells in G_2-M, inhibition of cyclin A levels, and hypophosphorylation of pRb at Ser^{249} and Thr^{252} are consistent with inhibition of CDK1 activity (38).

PHA-848125 showed significant antitumor activity in a wide range of human s.c. implanted xenograft tumors. Notably, the compound was effective in experimental models that more closely resemble human cancers than do xenografts, such as primary human disseminated leukemias in SCID mice and the rat carcinogen-induced mammary tumor (DMBA). In this latter model, following the guidelines used by clinicians to score response in solid tumors (39), we observed not only stasis but also tumor regression (with a "partial response" in 20–50% of evaluated tumors) and we believe this may be a significant finding in comparison with other latest-generation CDKIs. Several "evolved" CDK2 inhibitors, such as R547 (40), P276-00 (41), AT7519 (42), and AZD5438 (43), are reported to be in late preclinical or clinical testing, but we believe PHA-848125 is unique in possessing the combined properties reported here of good oral bioavailability, capacity to induce tumor regression, and flexibility of treatment scheduling, as shown in the DMBA-induced mammary carcinoma model. Notably, in all preclinical efficacy experiments, PHA-848125 was well tolerated without overt signs of toxicity.

In vivo mechanism of action of PHA-848125 was evaluated in the A2780 xenograft model, analyzing tumor biopsies by immunohistochemistry and RT-PCR for markers of CDK inhibition. Modulation of protein markers related to CDK activity and of E2F-regulated genes was fully coherent with observations we made *in vitro* using cell lines treated with the compound.

Moreover, the persistence of these modulations in the A2780 *in vivo* model following long-term treatment with

Published OnlineFirst August 3, 2010; DOI: 10.1158/1535-7163.MCT-10-0190

PHA-848125 allowed us to correlate the activity of the compound with its mode of action markers and has prompted the use of these biomarkers in phase I clinical studies.

The application of a pharmacokinetic/pharmacodynamic model for predicting TGI in mice also allowed us to estimate expected active doses in man and selection of the schedules that are currently being used in clinical trials. Specifically, we identified a target plasma concentration for tumor eradication of 2.4 μmol/L, which is close to the plasma concentration (1.47 ± 0.51 μmol/L) achieved in patients during a phase I dose escalation study at 150 mg/m^2 for 7 consecutive days in a 2-week cycle, eventually selected as the recommended phase II dose (44).

In addition to inhibiting CDK activity, PHA-848125 also potently inhibits members of the TRK kinase family. This may be significant when considering that we also observed activity in cell lines in which the pRb pathway is compromised through mutated, null, or nonfunctional pRb status, suggesting that in certain contexts, compound activity may depend on inhibition not solely of CDKs but rather of TRK family members, in particular TRKA. In the DU-145 human prostate carcinoma line, for example which has mutated Rb, but which expresses functional TRKA (27), the compound was able to inhibit NGF-induced phosphorylation of TRKA as well as its downstream signaling events.

Despite the fact that TRKA was one of the first transforming oncogenes identified, its role in tumorigenesis has been clearly established only in the last decade. In fact, constitutive activation of TRKs has been detected in several tumor types, including leukemias (45), and a novel alternative splicing variant with constitutive oncogenic potential has been recently described in neuroblastoma (46).

Somatic rearrangements of TRKA, producing chimeric oncogenes with constitutive tyrosine kinase activity, have been detected in a consistent fraction of papillary thyroid tumors (18), and an autocrine loop involving TRKA and NGF has been associated with tumor progression in prostate, ovarian, pancreatic, and breast cancer (20–24).

Interestingly, recent reports have shown that in some tumor types, the overexpression of both NGF and TRKA is associated with cancer-related pain syndrome (46, 47). TRKA is further implicated in pain sensation from studies on subjects with congenital insensitivity to pain with anhydrosis, a rare genetic disorder in which pain perception is lacking, and for which the underlying genetic defect has recently been pinpointed to loss-of-function mutations of the TRKA gene (48). This opens up the intriguing possibility that in appropriate tumor settings, a TRKA inhibitor might have the dual effect of controlling tumor growth/invasion and reducing pain symptomatology (49). First-generation compounds targeting the TRK/neurotrophin pathway, such as CEP-701 and AZD6918, despite their promising preclinical profiles, have been disappointing in phase I studies, due either to poor activity/selectivity or to unfavorable pharmacokinetic properties (50).

In summary, the *in vivo* efficacy of PHA-848125 against a large spectrum of tumors strongly supports our hypothesis that CDK/TRK dual inhibition could be considered a novel and rational targeted approach to cancer treatment, and considering its oral bioavailability, optimal tolerability, and pharmacokinetic properties, we believe that this drug holds promise for future clinical studies.

Disclosure of Potential Conflicts of Interest

No potential conflicts of interest were disclosed.

Acknowledgments

We thank Valter Croci, friend and colleague, who efficiently coordinated *in vivo* experiments and uplifted all with his smile. This paper is dedicated to his memory.

The costs of publication of this article were defrayed in part by the payment of page charges. This article must therefore be hereby marked *advertisement* in accordance with 18 U.S.C. Section 1734 solely to indicate this fact.

Received 02/25/2010; revised 05/25/2010; accepted 05/31/2010; published OnlineFirst 08/03/2010.

References

1. Sherr CJ, Roberts JM. Living with or without cyclins and cyclin-dependent kinases. Genes Dev 2004;18:2699–711.
2. Malumbres M, Barbacid M. To cycle or not to cycle: a critical decision in cancer. Nat Rev Cancer 2001;1:222–31.
3. Malumbres M, Barbacid M. Cell cycle, CDKs and cancer: a changing paradigm. Nat Rev Cancer 2009;9:153–66.
4. Ortega S, Malumbres M, Barbacid M. Cyclin D-dependent kinases, INK4 inhibitors and cancer. Biochim Biophys Acta 2002;1602:73–87.
5. Benson C, Kaye S, Workman P, Garrett M, Walton M, De Bono J. Clinical anticancer drug development: targeting the cyclin-dependent kinases. Br J Cancer 2005;92:7–12.
6. Swanton C. Cell-cycle targeted therapies. Lancet Oncol 2004;5:27–36.
7. Slingerland J, Pagano M. Regulation of the Cdk inhibitor p27 and its deregulation in cancer. J Cell Physiol 2000;183:10–7.
8. Desdouets C, Bréchot C. p27: a pleiotropic regulator of cellular phenotype and a target for cell cycle dysregulation in cancer. Pathol Biol 2000;48:203–10.
9. Ortega S, Prieto I, Odajima J, et al. Cyclin-dependent kinase 2 is essential for meiosis but not for mitotic cell division in mice. Nat Genet 2003;35:25–31.
10. Santamaria D, Barriere C, Cerqueira A, et al. CDK1 is sufficient to drive the mammalian cell cycle. Nature 2007;448:811–5.
11. Tetsu O, McCormick F. Proliferation of cancer cells despite CDK2 inhibition. Cancer Cell 2003;3:233–45.
12. Campaner S, Doni M, Hydbring P, et al. Cdk2 suppresses cellular senescence induced by the c-myc oncogene. Nat Cell Biol 2010;12:54–9.
13. Berthet C, Aleem E, Coppola V, Tessarollo L, Kaldis P. Cdk2 knockout mice are viable. Curr Biol 2003;13:1775–85.
14. Mendez J. Cell proliferation without cyclin E-Cdk2. Cell 2003;114:398–9.
15. Kozar K, Ciemerych MA, Rebel VI, et al. Mouse development and cell proliferation in the absence of D-cyclins. Cell 2004;118:477–91.
16. McInnes C. Progress in the evaluation of CDK inhibitors as anti-tumor agents. Drug Discov Today 2008;13:875–81.

Published OnlineFirst August 3, 2010; DOI: 10.1158/1535-7163.MCT-10-0190

17. Barbacid M. The Trk family of neurotrophin receptors. J Neurobiol 1994;25:1386–403.
18. Pierotti MA, Greco A. Oncogenic rearrangements of the NTRK1/NGF receptor. Cancer Lett 2006;232:90–8.
19. Lannon CL, Sorensen PH. ETV6-NTRK3: a chimeric protein tyrosine kinase with transformation activity in multiple cell lineages. Semin Cancer Biol 2005;15:215–23.
20. Festuccia C, Muzi P, Gravina GL, et al. Tyrosine kinase inhibitor CEP-701 blocks the NTRK1/NGF receptor and limits the invasive capability of prostate cancer cells *in vitro*. Int J Oncol 2007;30:193–200.
21. Ketterer K, Rao S, Friess H, Weiss J, Büchler MW, Korc M. Reverse transcription-PCR analysis of laser-captured cells point to potential paracrine and autocrine actions of neurotrophins in pancreatic cancers. Clin Cancer Res 2003;9:5127–36.
22. Lagadec C, Meignan S, Adriaenssens E, et al. TrkA overexpression enhances growth and metastasis of breast cancer cells. Oncogene 2009;28:1960–70.
23. Davidson B, Reich R, Lazarovici P, et al. Expression and activation of the nerve growth factor receptor TrkA in serous ovarian carcinoma. Clin Cancer Res 2003;9:2248–59.
24. Montano X, Djamgoz M. Epidermal growth factor, neurotrophins and the metastatic cascade in prostate cancer. FEBS Lett 2004;571:1–8.
25. Brasca MG, Albanese C, Amici R, et al. 6-Substituted pyrrolo[3,4-*c*] pyrazoles: an improved class of CDK2 inhibitors. Chem Med Chem 2007;2:841–52.
26. Brasca MG, Amboldi N, Ballinari D, et al. Identification of *N*,1,4,4-tetramethyl-8-{[4-(4-methylpiperazin-1-yl)phenyl]amino}-4,5-dihydro-1*H*-pyrazolo[4,3-*h*]quinazoline-3-carboxamide (PHA-848125), a potent, oral available cyclin dependent kinase inhibitor. J Med Chem 2009;52:5152–63.
27. Weeraratna AT, Arnold JT, George DJ, DeMarzo A, Isaacs JT. Rational basis for Trk inhibition therapy for prostate cancer. Prostate 2000;45:140–8.
28. Pevarello P, Brasca MG, Amici R, et al. 3-Aminopyrazole inhibitors of CDK2/cyclin A as antitumor agents. 1. Lead finding. J Med Chem 2004;47:3367–80.
29. Carpinelli P, Ceruti R, Giorgini ML, et al. PHA-739358, a potent inhibitor of Aurora kinases with a selective target inhibition profile relevant to cancer. Mol Cancer Ther 2007;6:3158–68.
30. Radaelli E, Ceruti R, Patton V, et al. Immunohistopathological and neuroimaging characterization of murine orthotopic xenograft models of glioblastoma multiforme recapitulating the most salient features of human disease. Histol Histopathol 2009;24:879–91.
31. Simeoni M, Magni P, Cammia C, et al. Predictive pharmacokinetic-pharmacodynamic modeling of tumor growth kinetics in xenograft models after administration of anticancer agents. Cancer Res 2004;64:1094–101.
32. Jang TJ, Kang MS, Kim DH, Lee JI, Kim JR. Increased expression of cyclin D1, cyclin E and p21 (Cip1) associated with decreased expression of p27(Kip1) in chemically induced rat mammary carcinogenesis. Jpn J Cancer Res 2000;91:1222–32.
33. Golay J, Di Gaetano N, Amico D, et al. Gentuzumab ozogamicin (Mylotarg) has therapeutic activity against $CD33^+$ acute lymphoblastic leukaemias *in vitro* and *in vivo*. Br J Haematol 2005;128:310–7.
34. Giavazzi R, Di Berardino C, Garofalo A, et al. Establishment of human acute myelogenous leukemia lines secreting interleukin-1β in SCID mice. Int J Cancer 1995;61:280–5.
35. Davies B, Morris T. Physiological parameters in laboratory animals and humans. Pharm Res 1993;10:1093–5.
36. Zarkowska T, Mittnacht S. Differential phosphorylation of the retinoblastoma protein by G_1/S cyclin-dependent kinases. J Biol Chem 1997;272:12738–46.
37. Knudsen ES, Wang JYJ. Differential regulation of retinoblastoma protein function by specific cdk phosphorylation sites. J Biol Chem 1996;271:8313–20.
38. Hassler M, Singh S, Yue WW, et al. Crystal structure of the retinoblastoma protein N domain provides insight into tumor suppression, ligand interaction, and holoprotein architecture. Mol Cell 2007;28: 371–85.
39. Eisenhauer EA, Therasse P, Bogaerts J, et al. New response evaluation criteria in solid tumours: revised RECIST guideline (version 1.1). Eur J Cancer 2009;45:228–47.
40. DePinto W, Chu X, Yin X, et al. *In vitro* and *in vivo* activity of R547: a potent and selective cyclin-dependent kinase inhibitor currently in phase I clinical study. Mol Cancer Ther 2006;5:2644–58.
41. Joshi KS, Rathos MJ, Mahajan P, et al. P276-00, a novel Cyclin-dependent inhibitor induces G_1-G_2 arrest, shows antitumor activity on cisplatin-resistant cells and significant *in vivo* activity in tumor models. Mol Cancer Ther 2007;6:926–34.
42. Squires MS, Feltell RE, Wallis NG, et al. Biological characterization of AT7519, a small-molecule inhibitor of cyclin-dependent kinases, in human tumor cell lines. Mol Cancer Ther 2009;8:324–32.
43. Byth KF, Thomas A, Hughes G, et al. AZD5438, a potent oral inhibitor of cyclin-dependent kinases 1, 2 and 9 leads to pharmacodynamic changes and potent antitumor effects in human xenografts. Mol Cancer Ther 2009;8:1856–66.
44. Tibes R, Jimeno A, Von Hoff D. Phase I dose escalation study of the oral multi-CDK inhibitor PHA-848125 [abstract 3531]. ASCO Annual Meeting Proceedings. J Clin Oncol 2008;26:3531.
45. Reuther GW, Lambert QT, Caligiuri MA, Der CD. Identification and characterization of an activating TrkA deletion mutation in acute myeloid leukemia. Mol Cell Biol 2000;20:8655–66.
46. Tacconelli A, Farina AR, Cappabianca I, Giulino A, Mackay AR. Alternative TrkAIII splicing: a potential regulated tumor-promoting switch and therapeutic target in neuroblastoma. Future Oncol 2005;1:689–98.
47. Zhu Z, Friess H, DiMola F, et al. Nerve growth factor expression correlates with perineural invasion and pain in human pancreatic cancer. J Clin Oncol 1999;17:2419–28.
48. Melamed I, Levy J, Parvari R, Gelfand EW. A novel lymphocyte signaling defect: trkA mutation in the syndrome of congenital insensitivity to pain and anhidrosis (CIPA). J Clin Immunol 2004;24: 441–8.
49. Halvorson KG, Kubota K, Sevcik MA, et al. A blocking antibody to nerve growth factor attenuates skeletal pain induced by prostate tumor cells growing in bone. Cancer Res 2005;65:9426–35.
50. Morgensztern D, Belani CP. Novel cytotoxic agents. J Thorac Oncol 2009;4:S1082–3.

Published OnlineFirst August 3, 2010; DOI: 10.1158/1535-7163.MCT-10-0190

Molecular Cancer Therapeutics

Dual Targeting of CDK and Tropomyosin Receptor Kinase Families by the Oral Inhibitor PHA-848125, an Agent with Broad-Spectrum Antitumor Efficacy

Clara Albanese, Rachele Alzani, Nadia Amboldi, et al.

Mol Cancer Ther 2010;9:2243-2254. Published OnlineFirst August 3, 2010.